

Study on the Evolution of a Northeast China Cold Vortex during the Spring of 2010

FU Shen-Ming¹, SUN Jian-Hua², and QI Lin-Lin³

¹ International Center for Climate and Environment Sciences (ICCES), Institute of Atmospheric Physics, Chinese Academy of Sciences, Beijing 100029, China

² Laboratory of Cloud-Precipitation Physics and Severe Storms (LACS), Institute of Atmospheric Physics, Chinese Academy of Sciences, Beijing 100029, China

³ Institute of Aeronautical Meteorology and Chemical Defense, Equipment Academy of Air Force, Beijing 100085, China

Received 23 September 2013; revised 7 November 2013; accepted 19 November 2013; published 16 March 2014

Abstract Based on the final analysis data with horizontal resolution of $1^\circ \times 1^\circ$ (four times a day) from the National Centers for Environmental Prediction (NCEP), a typical Northeast China cold vortex (NCCV) during the spring of 2010 was examined with the quasi-Lagrange-form eddy flux circulation (EFC) budget equation. Results indicated that the mechanisms that account for the development, maintenance, and attenuation of the cyclone varied with levels and stages. Displacement of the cyclone and transports by background environmental circulations dominated the variation of the cyclone in the middle and upper levels, whereas displacement and divergence associated with the cyclone dominated the evolution of the NCCV in the middle and lower levels. Moreover, interactions between the NCCV and other subsynoptic weather systems were important for the development of the cyclone, and the pattern of background environmental circulations was also important for the evolution of the NCCV, since the cyclone enhanced (weakened) as it moved from areas of low (high) vorticity to high (low) ones.

Keywords: Northeast China cold vortex, quasi-Lagrange-form eddy flux circulation budget

Citation: Fu, S.-M., J.-H. Sun, and L.-L. Qin, 2014: Study on the evolution of a northeast China cold vortex during the spring of 2010, *Atmos. Oceanic Sci. Lett.*, 7, 149–156, doi:10.3878/j.issn.1674-2834.13.0077.

1 Introduction

Cut-off lows (Hsieh, 1949; Price and Vaughan, 1992; Bell and Keyer, 1993; Trigo et al., 1999; Nieto et al., 2005) originating over Northeast China which mainly remain in the region of $36\text{--}60^\circ\text{N}$, $115\text{--}145^\circ\text{E}$, and which are accompanied by a cold core in the middle troposphere, are defined as the Northeast China cold vortex (NCCV) by Chinese meteorologists (Zheng et al., 1992). Temporally, NCCVs can occur throughout the year and their influences reach a maximum in summer (Sun et al., 1994; Zhao and Sun, 2007); spatially, NCCVs can influence Northeast China, Korea, East Russia, and even Japan, causing intense convective activities and heavy rainfall

events, as well as low temperatures and cold damage (He et al., 2006; Zhao and Sun, 2007; Zhang and Li, 2009).

Since the NCCV is an important weather system in East Asia, many efforts have been made to understand this kind of cyclone, including the climatological and statistical features of NCCVs (Liu et al., 2002; He et al., 2006); background environmental conditions favorable for the formation and maintenance of NCCVs (Liu et al., 2002; He et al., 2006); disaster weathers associated with NCCVs (Qiao et al., 2007; Zhao and Sun, 2007; Zhang et al., 2008); evolution mechanisms of NCCVs (Mao and Qu, 1997; Xia et al., 2012); and the relationships between NCCVs and other weather systems (Liu et al., 2002; He et al., 2006).

Although it is known that the background environment and other subsynoptic weather systems are important to the variations of the NCCVs (He et al., 2006; Qiao et al., 2007; Zhao and Sun, 2007), the details and mechanisms of an NCCV's interaction with the background environment and other subsynoptic weather systems are still vague. Therefore, the purpose of this study is to investigate the NCCV's interactions with the background environment and other weather systems and to understand the formation and evolution of the NCCV from a circulation perspective. The primary diagnostic tool employed in this paper is the eddy flux circulation (EFC) budget equation (Davis and Galarneau, 2009), which is a very useful tool for diagnosing the evolution of vortices and interactions among vortices and other systems.

2 Data and methodology

2.1 Data

Final analysis data with a horizontal resolution of $1^\circ \times 1^\circ$ at 6 hour intervals from the National Centers for Environmental Prediction (NCEP) were used for calculation and analysis in this paper. Conventional precipitation observation data obtained from the Chinese Meteorological Administration were also used in this study.

2.2 The EFC budget equation

The Euler form circulation budget equation derived by Davis and Galarneau (2009) was rewritten in the quasi-Lagrangian form as follows:

$$\frac{\delta C}{\delta t} = \mathbf{M}_h \cdot \nabla_h C - \bar{\eta} \tilde{\delta} A - \oint \eta \overline{V_h} \cdot \mathbf{n} dl$$

Motion-caused Stretching Background
Flux Flux

$$- \oint \eta' V'_h \cdot \mathbf{n} dl + \oint \omega (\mathbf{k} \times \frac{\partial V_h}{\partial p}) \cdot \mathbf{n} dl + \text{RES}, \quad (1)$$

Eddy Flux Tilting Residual term

where $\frac{\delta C}{\delta t}$ is a quasi-Lagrange variation of the circulation following the system; \mathbf{M}_h is the horizontal moving speed of the system; $\nabla_h = \frac{\partial}{\partial x} \mathbf{i} + \frac{\partial}{\partial y} \mathbf{j}$; $V_h = u\mathbf{i} + v\mathbf{j}$ is the horizontal wind field (u is the zonal wind and v is the meridional wind); $C = \oint V_h \cdot dl$ is the circulation along the system boundary; η is the absolute vorticity; $\tilde{\delta}$ is the system-area-averaged divergence; A is the area of the target system; ω is the vertical velocity in pressure coordinates; \mathbf{n} is the unit vector normal to the boundary line of the system; and \mathbf{k} is the unit vector in the vertical di-

rection; p is the pressure. Term RES includes friction and other sub-grid processes, and was calculated indirectly. Overbars are used to define the average value around the perimeter of the target system, and primes are used to denote perturbations from the average value. From the definition in Eq. (1), the Background Flux term can reveal the effects from background circulations and the Eddy Flux term can indicate influences from other subsynoptic weather systems.

3 Synoptic discussion

NCCVs were active during the spring of 2010, and in this study a typical case which occurred from 17 to 20 May 2010 and caused several heavy rainfall events was selected for detailed study. The evolution stages, key areas^① (KAs), and the vertical stretching of the cyclone are specified and shown in Table 1. These are determined by the precipitation (Fig. 1), geopotential height field, stream field, and positive vorticity (Fig. 2) associated with the cyclone.

During the formation stage, there was an eastward-moving short-wave trough to the east of China (Fig. 1a),

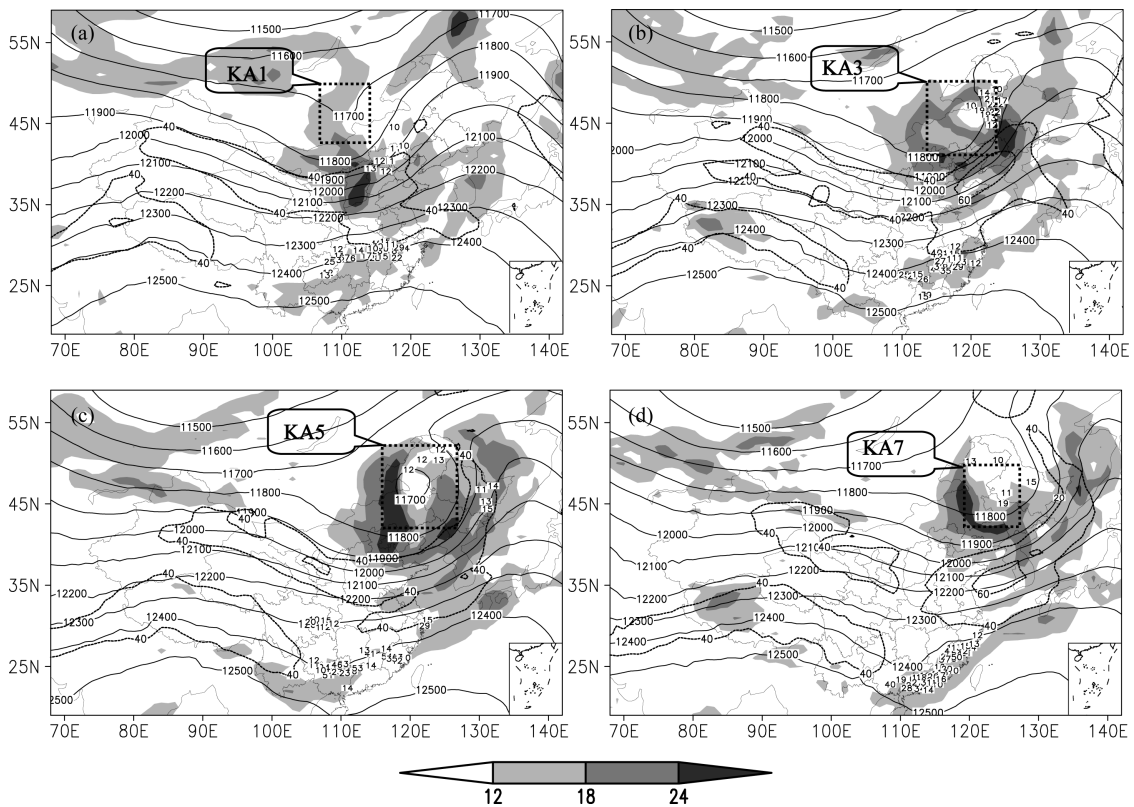


Figure 1 Geopotential height field (solid line, units: gpm), the upper-level jet (ULJ) (broken line, units: $m s^{-1}$) at 200 hPa, lower-level jet at 700 hPa (shaded, units: $m s^{-1}$), and 3-h precipitation (number, units: mm), where the dashed rectangles stand for KAs of the NCCV. (a) 0000 UTC 18 May, (b) 1200 UTC 18 May, (c) 0000 UTC 19 May, and (d) 1200 UTC 19 May 2010.

^①KAs were selected as follows: 1) to include the main body of the cyclone circulation (stream filed) and take the symmetry of the cyclone into consideration; 2) to include the main body of positive vorticity centers associated with the cyclone; 3) to exclude other systems surrounding the cyclone; and the most important one is 4) the KA-based calculations should be insensitive to relatively small changes to the KAs (small changes of $\pm 1^\circ$ (longitude/latitude) were made to the four boundary lines of the KAs, and the calculation results changed moderately with the dominant factors in Table 2 unchanged).

with a temperature trough behind it at 500 hPa (not shown) and an upper-level jet (ULJ) located around 40°N at 200 hPa. At 0000 UTC 18 May, the NCCV formed with a low center of 5480 gpm at 500 hPa (not shown) and an intense lower-level jet (LLJ) around the cyclone (Fig. 1a). The cut-off of the cold center from the temperature trough resulted in a cold center of -20°C associated with the cyclone at 500 hPa (not shown). After the NCCV formed, there was a temperature ridge above 300 hPa and a temperature trough below 350 hPa (Fig. 3a). Cold and warm advections associated with the cyclone were very intense, indicating the intense baroclinity of the system. Ascending motions were intense and mainly located to the east of KA1, corresponding to the precipitation (Fig. 1a). Moreover, to the east of the cyclone, an intense moisture convergence center formed, which favored the precipitation (not shown), and the water vapor was mainly transported by the southeast wind from the Bohai Sea and the Yellow Sea.

During the developing stage, the short-wave trough moved eastward and enhanced significantly, with a low center of 11700 gpm forming at 0000 UTC 19 May (Fig. 1c), indicating the intense vertical stretching of the cyclone (Table 1). The LLJ strengthened significantly and favored moisture transport for precipitation associated with the cyclone (Figs. 1b and 1c). The NCCV moved eastward with enlarging key areas and intense positive vorticity (Figs. 2c–g). Temperature advections enhanced due to the intensification of the north wind and south wind associated with the cyclone (Figs. 3b–f). Regions of ascending motion remained very intense and they moved eastward relative to the cyclone (Figs. 3b–f), indicating that the active regions of convection were mainly located to the east of the NCCV (Fig. 1). Precipitation associated with the cyclone first enhanced and then weakened, which was closely related to the variation of moisture transport; and the maximum 6-h precipitation of 23 mm during the whole cyclone lifetime appeared in this stage (Fig. 1b). The moisture was mainly transported by the southeast wind from the Bohai Sea, Yellow Sea, and Sea of Japan (not shown).

During the decaying stage, the short-wave trough moved eastward continuously but began to weaken (Fig.

1d); meanwhile, the ULJ and LLJ both weakened. The KAs of the NCCV shrank, and the positive vorticity center associated with the cyclone weakened quickly (Figs. 2h–j). Temperature advections associated with the cyclone weakened gradually (Figs. 3g and 3h), and so did the ascending motions, and the north and south wind centers. The moisture was mainly transported by the southeast wind from the Yellow Sea and the Sea of Japan, whereas the intensity of the moisture transport and convergence obviously weakened. Thus, the corresponding 6-h precipitation reduced significantly to less than 8 mm (not shown).

4 Results

4.1 Overview of the EFC budget and KA-averaged structure of the cyclone

The EFC budgets during life cycle of the NCCV were calculated using Eq. (1) at levels above 950 hPa (950 hPa is mainly above the topography within the KAs of the cyclone) and then averaged in the KAs of the cyclone. From Figs. 4b and 4c, the overall balance of the budget is generally good, with some discrepancies noted at 850 hPa and 400 hPa, after neglecting the residual term RES, thus, the budget results of EFC can be used for further research.

During the whole life cycle of the NCCV, the KA-averaged vorticity remained positive, with its maximum zone around 300 hPa (Fig. 4a), indicating that the NCCV was more intense in the upper troposphere (Fig. 3). In the formation and development stages, the convergence was mainly located in the middle and lower troposphere; and then in the decaying stage, the convergence weakened significantly and it was mainly located in the lower troposphere. Divergence was intense above 400 hPa during the formation and developing stages, and then it stretched downward to the lower troposphere and weakened remarkably during the decaying stage.

4.2 EFC budget of the NCCV during different stages

Before the formation, there was a positive vorticity center around 300 hPa, with a strong divergence center around 200 hPa and an obvious convergence center around 600 hPa (Fig. 4a). The transport of eddy vorticity

Table 1 Stages, KAs, and vertical stretching of the NCCV.

	Stages of the NCCV	The range of KAs	Vertical stretching
Before formation	1800 UTC 17 May	42–48°N, 108–115°E	
Formation	0000 UTC 18 May	42–48°N, 108–115°E	250–550 hPa
Developing stage	0600 UTC 18 May	41–49°N, 110–119°E	200–750 hPa
	1200 UTC 18 May	41–50°N, 114–123°E	250–900 hPa
	1800 UTC 18 May	41–51°N, 115–126°E	200–900 hPa
	0000 UTC 19 May	41–52°N, 116–127°E	200–900 hPa
Decaying stage	0600 UTC 19 May	42–51°N, 117–127°E	200–900 hPa
	1200 UTC 19 May	43–50°N, 120–128°E	250–900 hPa
	1800 UTC 19 May	44–50°N, 123–129°E	300–900 hPa
	0000 UTC 20 May	44–50°N, 123–129°E	

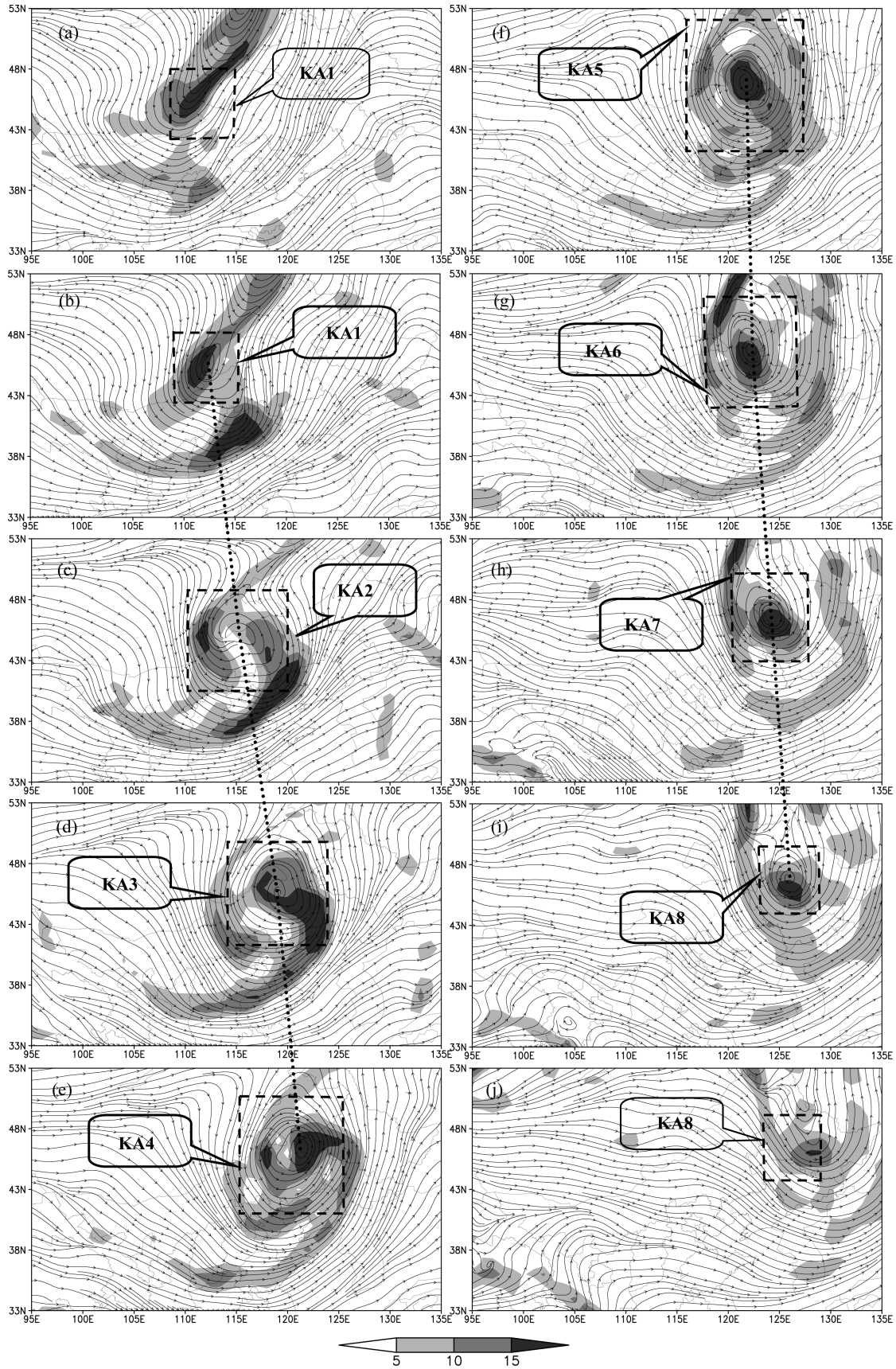


Figure 2 Streamline field and vorticity (shaded, units: 10^{-5} s^{-1}) at 500 hPa: (a) 1800 UTC 17 May; (b) 0000 UTC 18 May; (c) 0600 UTC 18 May; (d) 1200 UTC 18 May; (e) 1800 UTC 18 May; (f) 0000 UTC 19 May; (g) 0600 UTC 19 May; (h) 1200 UTC 19 May; (i) 1800 UTC 19 May; and (j) 0000 UTC 20 May 2010.

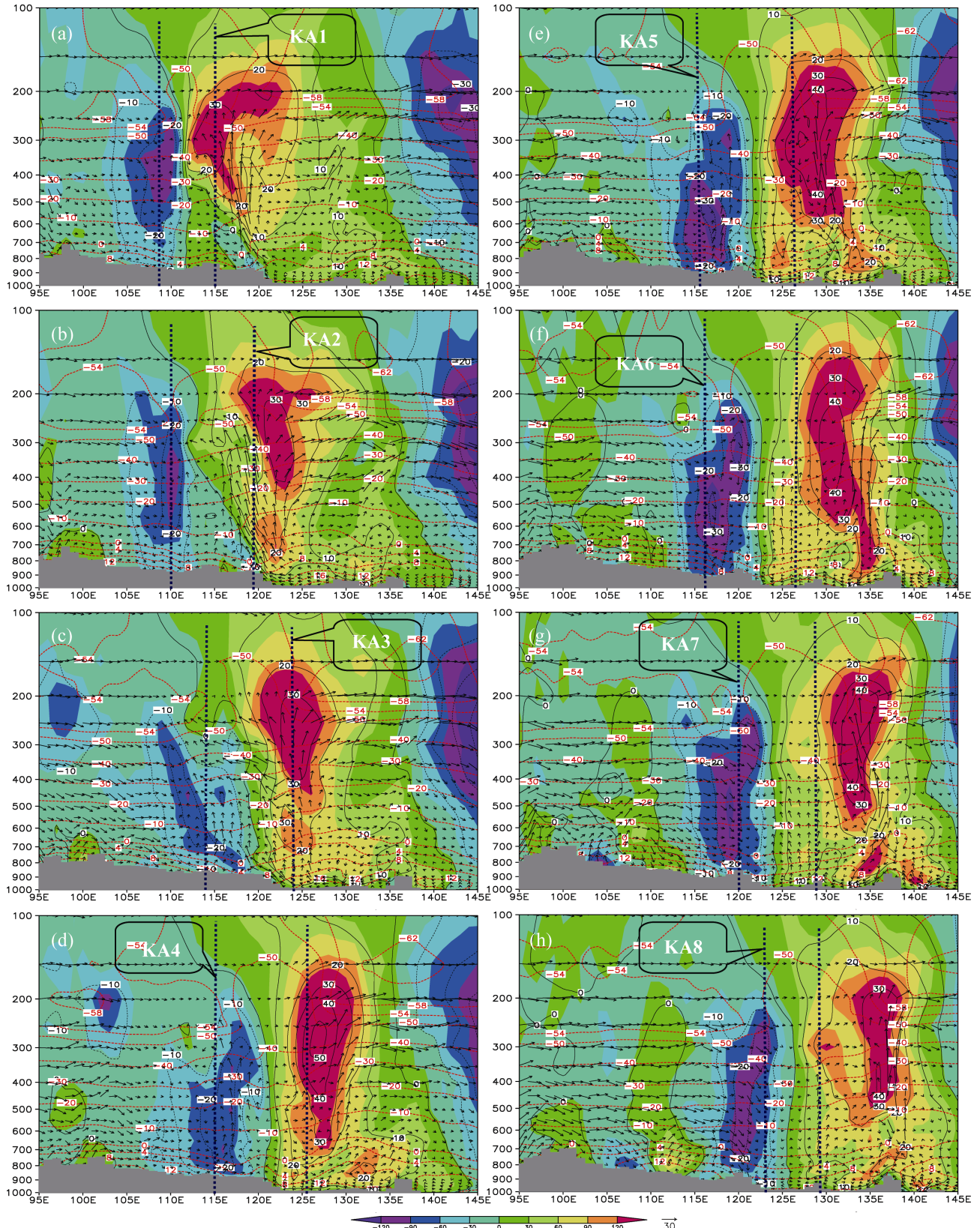


Figure 3 Cross sections along the central latitudes of the NCCV, where the shaded areas are horizontal advection of temperature (units: 10^{-5} K s^{-1}); the black solid and dashed lines are meridional velocity (units: m s^{-1}); red dashed lines are temperature (units: $^{\circ}\text{C}$); arrows are composed of zonal wind and vertical velocity (units: $\times 200 \text{ m s}^{-1}$); the gray at the bottom represents the topography; and the thick blue dotted lines represent the KAs of the NCCV. (a) 0000 UTC 18 May; (b) 0600 UTC 18 May; (c) 1200 UTC 18 May; (d) 1800 UTC 18 May; (e) 0000 UTC 19 May; (f) 0600 UTC 19 May; (g) 1200 UTC 19 May; and (h) 1800 UTC 19 May 2010.

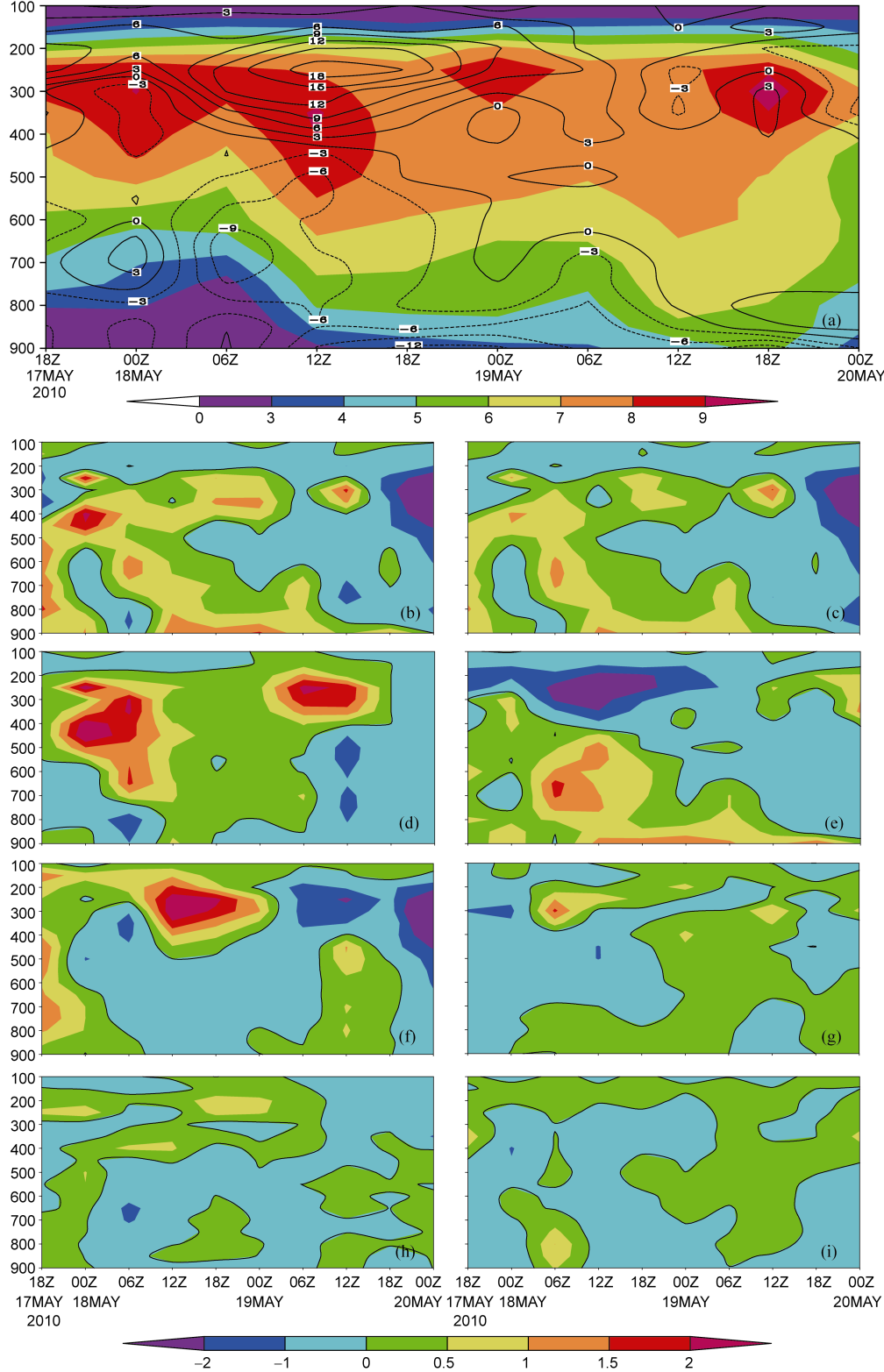


Figure 4 Cross sections of KA-averaged vorticity, divergence and results of the EFC budgets, where panel (a) depicts the averaged vorticity (shaded, units: 10^{-5} s^{-1}) and divergence (contours, units: 10^{-6} s^{-1}), (b) total effect of rhs terms of the EFC budget equation except for RES, (c) averaged Lagrangian variation, (d) Motion-caused Flux, (e) Stretching, (f) Background Flux, (g) Eddy Flux, (h) Tilting, and (i) RES. The solid line in (b)–(i) is of the value 0, and all the averaged terms of the EFC budgets are in units of 10^{-9} s^{-2} .

by background flows dominated the EFC budget (Fig. 4f). The Stretching term in the middle troposphere was also favorable for the formation of the NCCV due to convergence there (Figs. 4a and 4e). The Tilting term was con-

ducive to the enhancement of the cyclonic circulation around 250 hPa (Fig. 4h) due to the favorable configuration of the vertical wind shear and vertical motions (not shown). When the NCCV formed, the Motion-caused

Flux term dominated the budget of the EFC (Table 1), besides, the Stretching and Tilting terms were also mainly conducive to the development of the cyclone.

During the developing stage, the NCCV stretched downward to 900 hPa (Table 1). The Motion-caused Flux and Background Flux terms dominated the initial period of the developing stage in the middle and upper troposphere (Figs. 4d and 4f). Meanwhile, the Stretching and Motion-caused Flux terms dominated the downward stretching of the cyclone (Figs. 4d and 4e). Therefore, displacement was vital to the cyclone development. As the Motion-caused Flux term ($\mathbf{M}_h \cdot \nabla_h C$) showed, when the angle between \mathbf{M}_h and $\nabla_h C$ is less than 90°, or in other words, the cyclone moves from low vorticity areas to high ones, the Motion-caused Flux term is positive, which means the displacement favors the enhancement of the cyclonic circulation, whereas when the cyclone moves from high vorticity regions to low ones, this term is detrimental to the cyclone development. Moreover, a positive Eddy Flux in the upper and lower troposphere was mainly favorable for the cyclone development (Fig. 4g), and the tilting effects also favored the cyclone development in the upper troposphere (Fig. 4h).

During a later period of the developing stage, the Background Flux term which transported the positive vorticity into the KAs mainly by the southwest wind (not shown), and the Motion-caused Flux term dominated the cyclone development in the upper troposphere (Fig. 4f); and the Stretching term associated with the intense convergence (Fig. 4a) was the most favorable factor for the downward stretching of the NCCV (Fig. 4e). It should be noted that there was a maximum center of the Stretching term at 700 hPa around 0600 UTC 18 May (Fig. 4e), corresponding to an intense convergence center there (Fig. 4a). The convergence center formed suddenly (six hours before there was a divergence center at 700 hPa). But how did this convergence form over such a short period? At 0000 UTC 18 May, there was a trough with weak convergence and ascending motions within KA1 (not shown), and there was a meso-scale vortex with intense convergence and updraft to the east of the cyclone. Six hours later, the trough began to merge with the vortex as the NCCV moved eastward, thus, both the convergence and updraft within KA2 strengthened significantly (Figs. 3b and 4a). However, the enhancement of the ascending motions strengthened the divergence at high levels, resulting in an intensification of the divergence at 200 hPa (Fig. 4a), which was detrimental to the cyclone development at upper levels. Moreover, the Tilting term mainly favored the cyclone development in the upper troposphere (Fig. 4h), whereas the eddy transports favored the cyclone development in almost all the vertical stretching levels of the cyclone (Fig. 4g).

As discussed above, it is clear that development mechanisms of the NCCV were different among different levels. Displacement, transport by background circulations and other subsynoptic perturbations, and the tilting effects were all favorable for the cyclone development at middle-upper levels. The intense convergence due to the

merging of a trough with a meso-scale vortex, displacement, and eddy transports were all conducive to the cyclone development at middle-lower levels. The Motion-caused Flux term connected the upper level with the middle level, and the Stretching term linked the middle level with the lower level.

During the decaying stage, the convergence regions in the middle and lower troposphere reduced significantly with the convergence zones only remaining below 750 hPa (Fig. 4a). Meanwhile, the divergence areas in the middle and upper troposphere also weakened remarkably and stretched downward, with weak convergence zones appearing around 300 hPa (Fig. 4a). The decaying processes of the cyclone at different levels occurred in different ways: the Background Flux term dominated the dissipation of the NCCV in the middle and upper troposphere (Fig. 4f), whereas the Motion-caused Flux (Fig. 4d) and the Stretching (Fig. 4e) terms related to the divergence (Fig. 4a) dominated the cyclone dissipation at the middle-lower levels. In the middle and upper troposphere, the Motion-caused Flux (Fig. 4d) and the Stretching (Fig. 4e) terms related to the convergence (Fig. 4a), mainly acted to resist the decaying of the cyclone; whereas at the middle-lower levels, the Background Flux, Tilting, and Eddy Flux terms also resisted the decaying process of the NCCV.

5 Summary and conclusions

In this study, a typical NCCV that occurred from 17 to 20 May 2010 and caused several heavy rainfall events was investigated to understand its evolution and its interactions with the background environmental circulations and other subsynoptic systems.

The NCCV was closely related to a deep short-wave trough to the east of the Chinese mainland (Fig. 1) and there were intense ULJ and LLJ associated with the cyclone. The ULJ caused intense temperature advections, which favored the enhancement of baroclinity (that was very important to the NCCV's development); and the LLJ transported abundant moisture for precipitation associated with the cyclone. Intense convective activities mainly occurred to the east and/or north of the cyclone (Fig. 1), and moisture was mainly from the Bohai Sea, the Yellow Sea, and the Sea of Japan.

Cold temperature centers appeared within the KAs of the NCCV in the middle troposphere, which is the reason for the name "cold vortex," whereas, in the upper troposphere, warm centers associated with the temperature ridge were maintained. The NCCV is a kind of deeply developed baroclinic cyclone with intense temperature advections and a very deep vertical stretching (Table 1).

The NCCV developed from the top down, and it was very intense in the middle and upper troposphere. Except for the dominant factors shown in Table 2, it should be noted that the NCCV's interactions with other subsynoptic systems were also important to the evolution of the cyclone; and the displacement of the NCCV linked the middle-upper part and middle-lower part of the cyclone as a whole.

Table 2 Factors dominating the cyclone development during the formation and developing stages and factors dominated the cyclone attenuation during the decaying stage.

Levels	Formation stage		Developing stage		Decaying stage
	Before formation	Formation	Initial period	Latter period	
Middle-upper levels	Background Flux	Motion-caused Flux	Motion-caused Flux; Background Flux	Motion-caused Flux; Background Flux	Background Flux
Middle-lower levels	No NCCV	No NCCV	Motion-caused Flux; Stretching	Stretching	Motion-caused Flux; Stretching

Acknowledgements. This research was supported by the National Natural Science Foundation of China (Grant No. 41205027) and the National Key Basic Research Program of China (Grant No. 2012CB417201).

References

- Bell, G. D., and D. Keyser, 1993: Shear and curvature vorticity and potential-vorticity interchanges: Interpretation and application to a cutoff cyclone event, *Mon. Wea. Rev.*, **121**, 76–102.
- Davis, C. A., and J. G. Jr. Thomas, 2009: The vertical structure of mesoscale convective vortices, *J. Atmos. Sci.*, **66**, 686–704.
- He, J.-H., Z.-W. Wu, Z.-H. Jiang, et al., 2006: “Climate effect” of the northeast cold vortex and its influences on Meiyu, *Chinese Sci. Bull.* (in Chinese), **51**, 2803–2809.
- Hsieh, Y.-P., 1949: An investigation of a selected cold vortex over North America, *J. Meteor.*, **7**, 401–410.
- Liu, Z.-X., Y. Lian, Z.-T. Gao, et al., 2002 : Analyses of the northern Hemisphere circulation characters during northeast cold vortex persistence, *Chinese J. Atmos. Sci.* (in Chinese), **26**, 361–372.
- Mao, X.-M., and X.-B. Qu, 1997: Energetics analysis of a cold vortex in Northeast China, *Acta Meteor. Sinica* (in Chinese), **55**, 230–238.
- Nieto, R., L. Gimeno, and L. de la Torre, et al., 2005: Climatological features of cutoff low systems in the northern hemisphere, *J. Climate*, **18**, 3085–3103.
- Price, J. D., and G. Vaughan, 1992: Statistical studies of cut-off low systems, *Ann. Geophys.*, **10**, 96–102.
- Qiao, F.-X., S.-X. Zhao, and J.-H. Sun, 2007: Study of the vorticity and moisture budget of a northeast vortex producing heavy rainfall, *Climatic Environ. Res.* (in Chinese), **12**, 397–412.
- Sun, L., X.-Y. Zheng, and Q. Wang, 1994: The climatological characteristics of northeast cold vortex China, *Acta Meteor. Sinica* (in Chinese), **5**, 297–303.
- Trigo, I., T. D. Davies, and G. R. Bigg, 1999: Objective climatology of cyclones in the Mediterranean region, *J. Climate*, **12**, 1685–1696.
- Xia, R.-D., S.-M. Fu, and D.-H. Wang, 2012: On the vorticity and energy budgets of the cold vortex in Northeast China: A case study, *Meteor. Atmos. Phys.*, **118**, 53–64.
- Zhang, L.-X., and Z.-C. Li., 2009: A summary of research on cold vortex over Northeast China, *Climatic Environ. Res.* (in Chinese), **14**, 218–228.
- Zhang, Y., H.-C. Lei, and Z.-C. Qian, 2008: Analyses of formation mechanisms of a rainstorm during the declining phase of a northeast cold vortex, *Chinese J. Atmos. Sci.* (in Chinese), **32**, 481–498.
- Zhao, S. X., and J. H. Sun, 2007: Study on cut-off low-pressure systems with floods over northeast Asia, *Meteor. Atmos. Phys.*, **96**, 159–180.
- Zheng, X. Y., T. Z. Zhang, and R. H. Bai, 1992: *Rainstorm in Northeast China* (in Chinese), Metrorological Press, Beijing, 219pp.